Elucidating Molecule–Plasmon Interactions in Nanocavities with 2 nm Spatial Resolution and at the Single-Molecule Level

Fan-Li Zhang[+], Jun Yi[+], Wei Peng, Petar M. Radjenovic, Hua Zhang, Zhong-Qun Tian, and Jian-Feng Li*

Abstract: The fundamental understanding of the subtle interactions between molecules and plasmons is of great significance for the development of plasmon-enhanced spectroscopy (PES) techniques with ultrahigh sensitivity. However, this information has been elusive due to the complex mechanisms and difficulty in reliably constructing and precisely controlling interactions in well-defined plasmonic systems. Herein, the interactions in plasmonic nanocavities of film-coupled metallic nanocubes (NCs) are investigated. Through engineering the spacer layer, molecule–plasmon interactions were precisely controlled and resolved within 2 nm. Efficient energy exchange interactions between the NCs and the surface within the 1–2 nm range are demonstrated. Additionally, optical dressed molecular excited states with a huge Lamb shift of ≈ 7 meV at the single-molecule (SM) level were observed. This work provides a basis for understanding the underlying molecule–plasmon interaction, paving the way for fully manipulating light–matter interactions at the nanoscale.

The development of plasmon-enhanced spectroscopy (PES) techniques with ultrahigh sensitivity, including surface-enhanced Raman scattering (SERS) and surface-enhanced fluorescence (SEF), plays an important role in surface analysis and nanotechnologies.[1] These PES techniques can provide abundant molecular information about chemical reactions in a spectral form.[2] In order to obtain large enhancements of molecular spectroscopy, much attention has been concentrated on the construction of plasmonic nanostructures.[3] One of the most attractive plasmonic nanostructures is the nanoparticle-on-mirror (NPoM), which generates strongly confined gap plasmons between the two opposing metal surfaces.[4] Such plasmonic nanostructures provide significant electromagnetic field enhancement, and abundant optical phenomena of PES have been demonstrated. For example, the enhanced absorption cross-section makes it a perfect absorber surface.[5] Due to the extreme field confinement and enhancement in these plasmonic nanostructures, fast spontaneous emission, as well as strongly enhanced fluorescence and Raman signals, have been observed.[6] The strong couplings between plasmons and molecules at room temperature have been also demonstrated recently.[7]

Great progress has been made in PESs in recent years which has been applied in many fields, such as single-molecule (SM) electrochemistry with SEF,[8] and in situ Raman spectroscopy of single-crystal surfaces.[9] The behavior of PESs are critically dependent on subtle interactions between molecules and plasmons, such as perturbative interactions which enable spectral reshaping in SERS and SEF;[10] molecule–plasmon optomechanical interactions which induce nonlinear behavior in SERS;[11] and strong molecule–plasmon coupling interaction activated photon correlations in emitted photons.[12] Unraveling the complex mechanisms and interactions in these coupled systems requires the reliable construction of a well-defined plasmonic system with precise methods for tuning the plasmon resonance as well as the molecule–plasmon interaction strengths.

Herein, we describe a facile and novel approach for understanding and manipulating molecule–plasmon interactions in highly confined plasmonic nanocavities, which consisted of individual Ag nanocubes (NCs) coupled to an Au film. These nanocavities were highly tunable via adjusting the thickness of a polymer electrolyte spacer layer (PE layer) (see the Supporting Information for more details). Molecule–plasmon interactions could be precisely controlled through fine-tuning the position of embedded molecules within this spacer layer. By comparing the molecular-position-dependent SERS and SEF spectral intensities, we demonstrate efficient energy-exchange processes between molecules and plasmons, which were highly dependent on the coupling distance with a spatial resolution down to 1 nm. Additionally, a huge SM Lamb shift of 7 meV in the nanocavities via a SM fluorescence series was observed, revealing the interaction-induced optical dressing of molecular excited states at the SM level, as well as SM dynamics at room temperature.

The sample structure is depicted in Figure 1a and consists of chemically synthesized Ag NCs with an average size of 75 ± 3 nm (Figure 1b) and an ultraflat Au film (see Figure S2), separated by PE spacer layers. Probe molecules were embedded at different positions in the PE layers. Before the embedding process, the probe molecules were first linked to poly(allylamine)hydrochloride (PAH) through an amidation reaction. Then, the modified PAH solution was diluted to

[*] F. L. Zhang,[+] J. Yi,[+] W. Peng, Dr. P. M. Radjenovic, Prof. H. Zhang, Prof. Z. Q. Tian, Prof. J. F. Li
MOE Key Laboratory of Spectrochemical Analysis and Instrumentation, State Key Laboratory of Physical Chemistry of Solid Surfaces,*i*ChEM, College of Chemistry and Chemical Engineering
College of Materials, Xiamen University
Xiamen, 361005 (China)
E-mail: Li@xmu.edu.cn

Prof. J. F. Li
Shenzhen Research Institute of Xiamen University
Shenzhen, 518000 (China)

[+] These authors contributed equally to this work.

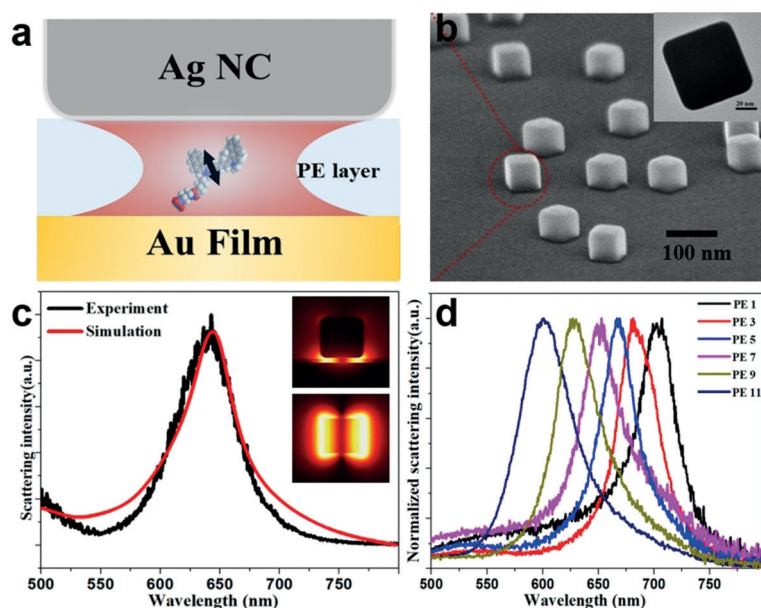Supporting information and the ORCID identification number(s) for the author(s) of this article can be found under:
https://doi.org/10.1002/anie.201906517.

Figure 1. a) Schematic of PES in a plasmonic nanocavity. b) SEM image of Ag NCs spread on Au film. The inset is a high-resolution TEM image of a Ag NC coated with a PVP shell. c) The measured (black curve) and simulated (red curve) dark-field scattering spectrum of an individual plasmonic nanocavity filled with seven PE layers. d) Normalized dark-field scattering of individual nanocavities with various numbers of PE layers.

a concentration of 3 mM with 1M NaCl solution (see the Supporting Information for details).

We used a home-built confocal dark-field microscope (see Figure S1) to characterize the plasmonic resonances of individual single nanocavities. Typical measured and calculated scattering spectra are shown in Figure 1c and are in good agreement. Under illumination, gap-plasmon modes are excited in the nanocavities and undergo a Fabry–Perot cavity-like resonance.[13] The simulated electric distribution presented in the inset reveals that the electric field is mainly confined at the edge of the nanocavities. The resonance energy of such nanocavities can be tuned by controlling either the size of the Ag NCs or the thickness of the assembled PE layers. For nanocavities with thinner PE layers, the resonance red-shifts to 700 nm, as shown in Figure 1d, which enables precise tuning of the resonance to cover the visible region.

To elucidate the interactions between molecules and plasmons in the nanocavities, the radiative properties of the molecule–cavity coupled system are investigated by monitoring their SERS and SEF behavior. We deposited seven layers of PE inside the cavity to tune the resonance (at ≈640 nm) to match with the excitation laser (at 633 nm). The cyanine 5.5-allophycocyanin (Cy5.5 APC) molecule was selected as a Raman probe for two reasons: First, the molecule is in resonance with the laser, resulting in strong resonance Raman signals for ideal detection; second, since the Stokes shift of

the molecules is large, overwhelming fluorescence background in the Raman signals can be avoided. In order to control the interactions between the probe molecule and plasmons, the molecules were precisely placed at various heights inside the nanocavity via layer-by-layer deposition (see Figure 2a; more details are given in the Supporting Information).

The measured Raman spectra from molecules at various positions are shown in Figure 2b. Two strong peaks centered at 578.8 cm⁻¹ and 727.3 cm⁻¹ are clearly observed, which are characteristic Raman peaks of Cy5.5 APC. For all observed Raman peaks, the Raman intensity decreased when the assembled molecules were located further away from the bottom layer of the nanocavity (i.e. adjacent to the Au film), while the intensity increased again when the molecules were closer to the top layer of the nanocavity (i.e. adjacent to the Ag NC). The integrated SERS peak intensity (peak at 578.8 cm⁻¹, see Figure S3 for all peaks) as a function of the molecules' position is summarized in Figure 2d and implies inhomogeneous interactions between molecules and plasmons in the nanocavity, showing vertical spatial resolution down to 1–2 nm. This can be explained by the inhomogeneous distribution of electric fields within the nanocavity. Since the excited gap-plasmons are confined to metal–spacer interfaces, they decay exponentially away from the interfaces.[14] As a result, molecules close to the interface experience larger electric field
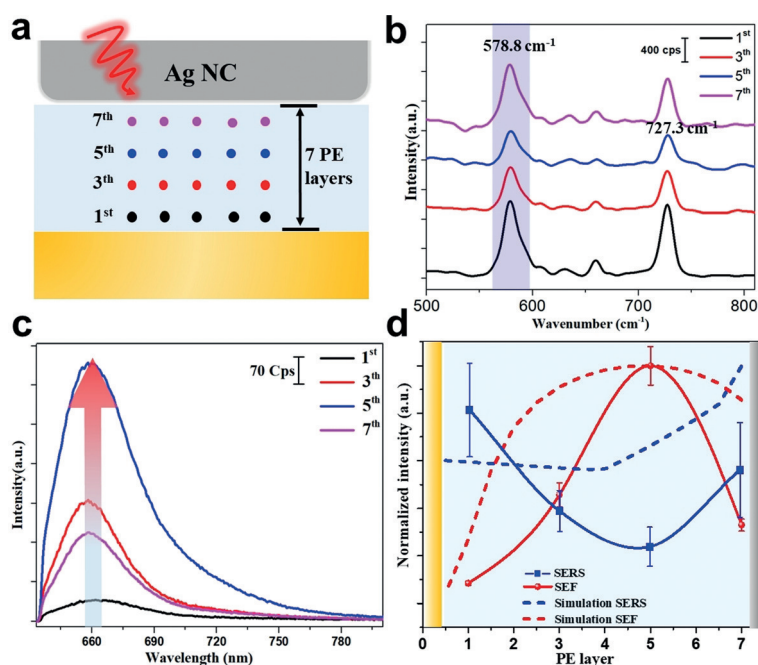

Figure 2. a) Schematic of molecules located at various positions within the nanocavity, marked as points with various colors, respectively. b) The measured Raman spectra from probes layer-by-layer in various positions. c) The measured fluorescence spectra of probes layer-by-layer in various positions. d) The normalized intensities of SERS and SEF peaks as a function of probe position.

enhancement and generate stronger SERS intensity signals. The simulated results from electric field inhomogeneity are consistent with those measured as shown in Figure 2d.

However, when the molecular fluorescence dominates in the nanocavity emission, the trend is reversed. For SEF measurements, we used a similar cyanine 5 (Cy5) probe molecule; its fluorescent Stokes shift is minor and its fluorescence peak is centered at 660 nm. The measured fluorescence signals show significant dependency on the vertical position of the probe molecules (Figure 2c). The strongest emission intensity originates from the center of the nanocavity and is weaker close to the Ag NC edges, opposite to what was observed with SERS. This contradicting plasmon enhancement phenomenon indicates that different optical interactions arise in SEF, that is, strong energy transfer processes between probe molecules and the cavity. As an intuitive explanation, energy can be exchanged via the dipole–dipole interactions between molecular dipoles and their image dipoles, similar to the Forster resonance energy transfer (FRET) process.[15] Therefore, molecules assembled near the Au film or Ag NCs experience weaker fluorescence emissions due to this strong energy transfer effect. A detailed discussion is provided in the Supporting Information (Figure S2). This was further confirmed by finite-element method (FEM) simulations. The spontaneous emission rate γ_{sp} and non-radiative decay rate γ_{nr} decrease rapidly as the distance between the probe molecule layer and Au film increases (Figure S5).

Interestingly, the emission signal from probe molecules close to the Au film (Figure 2c, 1st layer) is much weaker than that from near the Ag NC (7th layer), because in the former case energy is mainly coupled to the propagating surface plasmon mode of the Au film, which is less emissive. Since the efficiency of the energy transfer process is exponentially proportional to the molecule–cavity distance, the observed fluorescence intensity contrast is extremely sensitive to the molecule positions, with a vertical spatial resolution down to near 1 nm. However, this effect is insignificant in SERS because Raman scattering does not involve the relaxation of excited electrons and is thus almost instantaneous compared to fluorescence. Therefore, the energy exchange effect in SERS is strongly suppressed and only local field enhancements dominate the optical interactions.

More interestingly, the fluorescence emission spectra from molecules embedded at various positions also show slight Stokes shifts from 658 nm to 663 nm (see Figure S6). This phenomenon has been observed previously and is understood by three main mechanisms. First, the fluorescence emission can be reshaped by the nanocavities, known as the plasmon-reshaping effect;[16] second, molecular aggregation leads to inhomogeneous broadening of fluorescence signals;[17] third, variations of the local EM environment result in the shifts of the peaks.[18] Regarding the work herein, since the probed molecules are coupled with the same nanocavities, the first mechanism can be safely excluded. In order to minimize the intermolecular interactions and clarify the molecule–cavity interactions further SM fluorescence experiments have been carried out.

Figure 3a shows the fluorescence intensity trajectories as a function of measured time from a single Cy5 molecule, which was obtained via integrating the fluorescence peaks from 645 to 675 nm. In the first 7.2 s, the intensity is almost stable with minor fluctuations; after that, it suddenly drops to
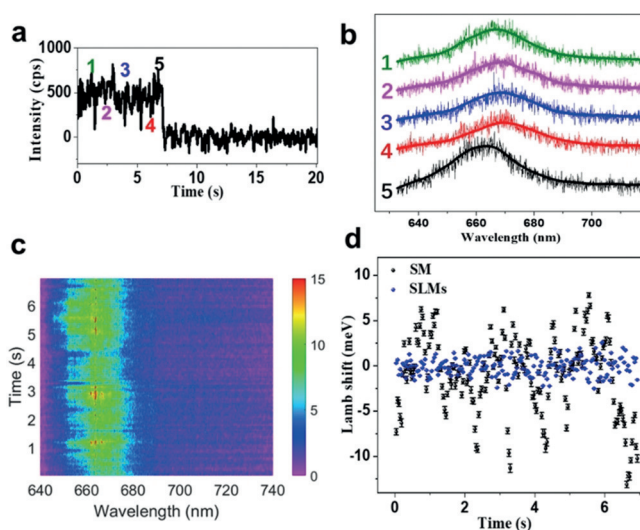

Figure 3. a) SM fluorescence intensity as a function of measured time. b) Five SM fluorescence spectra extracted from (a). c) Fluorescence time evolution contour plot of a SM in the nanocavity. d) Extracted Lamb shift of SM (black dots) and SLMs (blue dots) as a function of time.

zero and shows an abrupt intensity step due to photobleaching of the molecule. The single-step feature confirms the SM fluorescence event in the cavity.[19] Figure 3b shows five typical SM spectra extracted at various time intervals. Apparent random drifts in emission frequency are observed; this phenomenon reveals that the third mechanism dominates since only one molecule emits.

A complete time-evolution SM fluorescence series is shown in Figure 3c, reflecting the dynamics of the SM emission frequency. The peak energy, which was extracted via standard Gaussian fitting (Figure S6), shows a significant random drift in the emission energy accompanied by unexpected continuous blue-shifts. The rate of this systematic blue-shift is 2.21 meV s^{-1}, as evaluated from the linear fitting of the data. The shift of SM fluorescent energy indicates that the molecule–cavity interactions vary with time, which is usually interpreted as being due to fluctuations in the local EM environment or dynamic changes in molecules such as from molecular Brownian motion. However, this should not lead to a continuous blue-shift in spectra since molecular Brownian motions are intrinsically random.

To elucidate this effect, control experiments were performed by monitoring the fluorescence series of single-layer molecules (SLMs) within the same nanocavity (Figure S7B). For the SLMs in the nanocavity, the emission frequency statistics also show continuous blue-shifts, and the drift rate obtained by fitting is 2.06 meV s^{-1}, which is very close to the SM case described previously. This fact that this feature was seen in both SM and SLMs measurements implies that rather

than being due to molecular behavior, this continuous blue-shift actually arises from the dynamics of the cavity, that is, the photothermal effect inducing the thermal expansion of the nanocavities.[20] Both the PE layer and coated PVP protecting layers undergo thermal expansion under laser illumination, resulting in the thickness of the cavity increasing and causing a blue-shift in the cavity resonance energy.

We simulated the plasmonic resonance before and after thermal expansion of the PVP (Figure S8A). If the cavity experiences a thermal expansion of 2 nm, the cavity resonance blue-shifts by ≈ 15 nm, as observed experimentally. During the photothermal process, the plasmonic cavity survives and this thermal expansion is reversible. As demonstrated in Figure S8B, no variations are observed for the measured dark-field scattering before and after the laser excitation. After removing the linear-fitted blue-shifts, this difference thus reflects the dynamics of molecule–cavity interactions (Figure 3 d). While the peak shift remains within ± 1 meV in the SLM case, significant random drifts as large as ± 7 meV are observed in the SM case.

In the inhomogeneous plasmonic cavity, the molecular dipole experiences driving forces from its own field, which is the field that arrives back to the molecules after scattering by the cavity. This self-interaction results in a dressing of the molecular excited states, leading to a perturbation of the complex eigenfrequencies of the states. Variations in the real part of eigenfrequencies reflect the energy shift of the observed emission frequency, known as the Lamb shift;[21] while the change of the imaginary part leads to the modifications of the decay rate, identified as the Purcell effect.[22] Here we focus on the Lamb shift effect, the energy shift $\Delta\omega \propto -Re(\mu \bullet \boldsymbol{G}(\boldsymbol{r}, \boldsymbol{r}_1, \omega) \bullet \mu)$, in which μ is the molecular dipole moment and $\boldsymbol{G}(\boldsymbol{r}, \boldsymbol{r}_1, \omega)$ is the Green's function of the molecule–cavity system. This relation thus directly links the observed random frequency shifts to the molecular dynamics, for example, reflecting the random rotation or motion of molecules in the nanocavity.

Due to the averaging effect of multiple molecules, this random effect is suppressed in the SLM case. Thus, we simulated the detailed emission spectra of a SM located at different horizontal positions in the nanocavity. The extracted peak frequencies as shown in Figure 4 a show notable inhomogeneous features. Three typical calculated spectra from various molecular positions are shown in Figure 4 b. The emission frequency of molecules at edges of the cavity is 12 meV lower than from those at the center of the cavity, since at the edges the molecules experience stronger self-interaction. The ± 6 meV peak drift also is consistent with the experimental observations.

In conclusion, we have investigated the underlying interactions between molecules and nanocavities. The energy exchange channel between molecules and plasmons is observed and found to be highly sensitive to the molecular positions with a spatial resolution down to the nanometer scale. In addition, we demonstrate a huge room temperature Lamb shift of 7 meV at the SM level, revealing the optical dressing of molecular excited states at the SM level. Our results represent the first step toward fully understanding and manipulating the light–matter interactions at the nanoscale
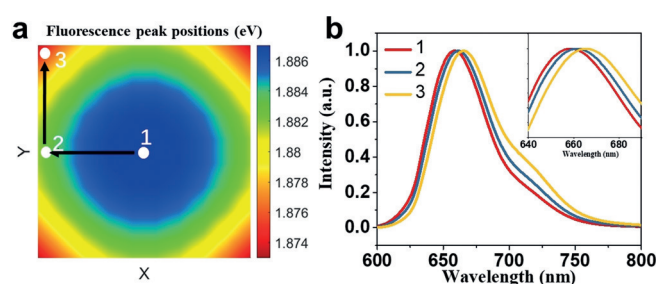

Figure 4. a) Maps of peak position of fluorescence as a function of molecule position within the nanocavity; three positions are labeled 1, 2, and 3. b) The corresponding fluorescence spectra in these positions. The inset shows a close-up of the peak region.

and open up the exploration for complex processes of SM sensing based on the resonant photonic cavity.

Acknowledgements

Conflict of interest

The authors declare no conflict of interest.

[1] a) S.-Y. Ding, J. Yi, J.-F. Li, B. Ren, Z.-Q. Tian, *Nat. Rev. Mater.* **2016**, *1*, 16021; b) J. F. Li, Y. F. Huang, Y. Ding, B. Ren, Z.-Q. Tian, *Nature* **2010**, *464*, 392.

[2] a) Z. Peng, Y. Chen, P. G. Bruce, Y. Xu, *Angew. Chem. Int. Ed.* **2015**, *54*, 8165–8168; *Angew. Chem.* **2015**, *127*, 8283–8286; b) W. Xie, B. Walkenfort, S. Schlücker, *J. Am. Chem. Soc.* **2013**, *135*, 1657–1660.

[3] a) K. J. Russell, T.-L. Liu, S. Cui, E. L. Hu, *Nat. Photonics* **2012**, *6*, 459; b) P. Zhan, T. Wen, Z. g. Wang, Y. He, J. Shi, T. Wang, X. Liu, G. Lu, B. Ding, *Angew. Chem. Int. Ed.* **2018**, *57*, 2846–2850; *Angew. Chem.* **2018**, *130*, 2896–2900; c) L. Xin, M. Lu, S. Both, M. Pfeiffer, M. J. Urban, C. Zhou, H. Yan, T. Weiss, N. Liu, K. Lindfors, *ACS Photonics* **2019**, *6*, 985–993; d) A. Kinkhabwala, Z. Yu, S. Fan, Y. Avlasevich, K. Müllen, W. Moerner, *Nat. Photonics* **2009**, *3*, 654; e) V. Giannini, A. I. Fernández-Domínguez, S. C. Heck, S. A. Maier, *Chem. Rev.* **2011**, *111*, 3888–3912; f) K. Liu, Y. Bai, L. Zhang, Z. Yang, Q. Fan, H. Zheng, Y. Yin, C. Gao, *Nano Lett.* **2016**, *16*, 3675–3681.

[4] a) J. J. Baumberg, J. Aizpurua, M. H. Mikkelsen, D. R. Smith, *Nat. Mater.* **2019**, https://doi.org/10.1038/s41563-019-0290-y;

b) M. Hu, A. Ghoshal, M. Marquez, P. G. Kik, *J. Phys. Chem. C* **2010**, *114*, 7509 – 7514; c) G.-C. Li, Q. Zhang, S. A. Maier, D. J. N. Lei, *Nanophotonics* **2018**, *7*, 1865 – 1889; d) T. Maurer, P.-M. Adam, G. J. N. Lévêque, *Nanophotonics* **2015**, *4*, 363 – 382.

[5] a) A. Moreau, C. Ciracì, J. J. Mock, R. T. Hill, Q. Wang, B. J. Wiley, A. Chilkoti, D. R. J. N. Smith, *Nature* **2012**, *492*, 86; b) G. M. Akselrod, J. Huang, T. B. Hoang, P. T. Bowen, L. Su, D. R. Smith, M. H. J. A. M. Mikkelsen, *Adv. Mater.* **2015**, *27*, 8028 – 8034.

[6] a) F. Benz, M. K. Schmidt, A. Dreismann, R. Chikkaraddy, Y. Zhang, A. Demetriadou, C. Carnegie, H. Ohadi, B. de Nijs, R. Esteban, *Science* **2016**, *354*, 726 – 729; b) G. M. Akselrod, C. Argyropoulos, T. B. Hoang, C. Ciracì, C. Fang, J. Huang, D. R. Smith, M. H. J. N. P. Mikkelsen, *Nat. Photonics* **2014**, *8*, 835; c) R. Chikkaraddy, V. A. Turek, N. Kongsuwan, F. Benz, C. Carnegie, T. van de Goor, B. de Nijs, A. Demetriadou, O. Hess, U. F. Keyser, J. J. Baumberg, *Nano Lett.* **2018**, *18*, 405 – 411; d) Y. Fu, J. Zhang, J. R. Lakowicz, *J. Am. Chem. Soc.* **2010**, *132*, 5540 – 5541; e) S. Nie, S. R. Emory, *Science* **1997**, *275*, 1102 – 1106; f) M. Pelton, *Nat. Photonics* **2015**, *9*, 427.

[7] a) R. Chikkaraddy, B. De Nijs, F. Benz, S. J. Barrow, O. A. Scherman, E. Rosta, A. Demetriadou, A. Fox, O. Hess, J. J. J. N. Baumberg, *Nature* **2016**, *535*, 127; b) X. Chen, Y.-H. Chen, J. Qin, D. Zhao, B. Ding, R. J. Blaikie, M. Qiu, *Nano Lett.* **2017**, *17*, 3246 – 3251; c) J. Huang, A. J. Traverso, G. Yang, M. H. J. A. P. Mikkelsen, *ACS Photonics* **2019**, *6*, 838 – 843.

[8] W. Zhang, M. Caldarola, B. Pradhan, M. Orrit, *Angew. Chem. Int. Ed.* **2017**, *56*, 3566 – 3569; *Angew. Chem.* **2017**, *129*, 3620 – 3623.

[9] a) J.-C. Dong, X.-G. Zhang, V. Briega-Martos, J. M. Feliu, C. T. Williams, J.-F. Li, *Nat. Energy* **2019**, *4*, 60; b) Y.-F. Huang, P. J. Kooyman, M. T. Koper, *Nat. Commun.* **2016**, *7*, 12440.

[10] a) K.-Q. Lin, J. Yi, J.-H. Zhong, S. Hu, J. Aizpurua, *Nat. Commun.* **2017**, *8*, 14891; b) M. Ringler, A. Schwemer, M. Wunderlich, A. Nichtl, K. Kürzinger, T. Klar, J. Feldmann, *Phys. Rev. Lett.* **2008**, *100*, 203002.

[11] a) P. Roelli, C. Galland, N. Piro, T. J. Kippenberg, *Nat. Nanotechnol.* **2016**, *11*, 164; b) M. K. Schmidt, R. Esteban, A. González-Tudela, G. Giedke, J. Aizpurua, *ACS Nano* **2016**, *10*, 6291 – 6298; c) A. Lombardi, M. K. Schmidt, L. Weller, W. M.

Deacon, F. Benz, B. De Nijs, J. Aizpurua, J. J. Baumberg, *Phys. Rev. X* **2018**, *8*, 011016.

[12] a) C. Downing, J. L. Carreño, F. P. Laussy, E. Del Valle, A. Fernández-Domínguez, *Phys. Rev. Lett.* **2019**, *122*, 057401; b) R. Sáez-Blázquez, J. Feist, A. Fernández-Domínguez, F. García-Vidal, *Optica* **2017**, *4*, 1363 – 1367; c) O. S. Ojambati, R. Chikkaraddy, W. D. Deacon, M. Horton, D. Kos, V. A. Turek, U. F. Keyser, J. J. Baumberg, *Nat. Commun.* **2019**, *10*, 1049.

[13] J. B. Lassiter, F. McGuire, J. J. Mock, C. Ciracì, R. T. Hill, B. J. Wiley, A. Chilkoti, D. R. Smith, *Nano Lett.* **2013**, *13*, 5866 – 5872.

[14] a) B. Hecht, H. Bielefeldt, L. Novotny, Y. Inouye, D. Pohl, *Phys. Rev. Lett.* **1996**, *77*, 1889; b) P. Bharadwaj, A. Bouhelier, L. Novotny, *Phys. Rev. Lett.* **2011**, *106*, 226802.

[15] a) C. Yun, A. Javier, T. Jennings, M. Fisher, S. Hira, S. Peterson, B. Hopkins, N. Reich, G. Strouse, *J. Am. Chem. Soc.* **2005**, *127*, 3115 – 3119; b) Q. Hu, D. Jin, J. Xiao, S. H. Nam, X. Liu, Y. Liu, X. Zhang, N. X. Fang, *Proc. Natl. Acad. Sci. USA* **2017**, *114*, 10017 – 10022.

[16] a) B. Ding, C. Hrelescu, N. Arnold, G. Isic, T. A. Klar, *Nano Lett.* **2013**, *13*, 378 – 386; b) Z.-Q. Li, C. Zhang, P. Gu, M. Wan, P. Zhan, Z. Chen, Z. Wang, *Appl. Phys. Lett.* **2015**, *107*, 251105.

[17] H. Tong, Y. Hong, Y. Dong, M. Häußler, J. W. Lam, Z. Li, Z. Guo, Z. Guo, B. Z. Tang, *Chem. Commun.* **2006**, 3705 – 3707.

[18] F. Tam, G. P. Goodrich, B. R. Johnson, N. J. Halas, *Nano Lett.* **2007**, *7*, 496 – 501.

[19] a) A. Gaiduk, M. Yorulmaz, P. Ruijgrok, M. Orrit, *Science* **2010**, *330*, 353 – 356; b) R. Chikkaraddy, V. Turek, N. Kongsuwan, F. Benz, C. Carnegie, T. van de Goor, B. de Nijs, A. Demetriadou, O. Hess, U. F. Keyser, *Nano Lett.* **2018**, *18*, 405 – 411.

[20] W. Chen, S. Zhang, Q. Deng, H. Xu, *Nat. Commun.* **2018**, *9*, 801.

[21] A. Fragner, M. Göppl, J. Fink, M. Baur, R. Bianchetti, P. Leek, A. Blais, A. Wallraff, *Science* **2008**, *322*, 1357 – 1360.

[22] K.-D. Park, T. Jiang, G. Clark, X. Xu, M. B. Raschke, *Nat. Nanotechnol.* **2018**, *13*, 59.